DNIPRO UNIVERSITY of TECHNOLOGY 1899

Mining of Mineral Deposits
Volume 14 (2020), Issue 2, 16-24

MMD JOURNAL / MINING.IN.UA

UDC 622.271.332 https://doi.org/10.33271/mining14.02.016

Rock slope stability analysis using shear strength reduction technique (SSRT) – case histories

Wael R. Abdellah[1*], Mamdouh Y. Hussein[1], Said S. Imbabi[1]

[1]*Assiut University, Assiut, 71516, Egypt*

**Corresponding author: e-mail wael.abdellah80@gmail.com, tel. +201006816653*

Abstract

Purpose. This study aims to evaluate the slope stability of open pit comprising massive and jointed rock mass.

Methods. Mohr-Coulomb yield function (MC) with shear strength reduction technique (SSRT) are incorporated in finite element analysis (FEA) and four different slopes with varying geometry and geological structural features with an ultimate slope angle of 34° are analyzed using the two-dimensional FEA Program RS2D. The first slope comprises blocky rock mass; the second slope has a network of joints parallel to slope face; the third slope has a parallel joint networks dip out the slope face, and the last slope has a cross-joints network.

Findings. The critical strength reduction factor (CSRF) indicates whether the slope face is stable (if CSRF ≥ 1) or not. The minimum CSRF of 0.53 (e.g. compared to 0.55 for parallel joints dip out to the slope face, 0.58 for joints parallel to slope face and 0.65 with no joint existed) is obtained with cross-joints network existed. The CSRF (e.g., CSRF = 0.49) reduces when the MC slip criterion is adopted with the jointed rock mass.

Originality. This study attempts new stability indicator namely critical strength reduction factor (CSRF) embedded in shear strength reduction technique (SSRT), based on finite element (FEM) to assess the slope of open pit with respect to presence of geological discontinuities.

Practical implications. The slope stability of rock mass is significant to design parameters in open pit mines. Unexpected instability is eventually costly, hazardous to personnel/machinery, disrupted to the mining operation and time-consuming. Therefore, this study Provides a methodology for the application of shear strength reduction technique (SSRT) when evaluating the slope stability of open pit mines with respect to existence of geological features. As a result, the mine planners and engineers will be able to know a head of time when and where necessary support is needed.

Keywords: *open pit slope stability, shear strength reduction technique (SSRT), factor of safety (FS), critical strength reduction factor (CSRF)*

1. Introduction

Open pit mining is one of the most economical mining methods when extracting large volumes of mineral ore deposits, which can accommodate different size equipment. Scrapers and bucket wheel excavators are employed when excavating very soft rocks, draglines are used to excavate weak to medium strength rocks, while, trucks and shovels are commonly used to excavate weak to very strong rocks. The geometry of open pit (i.e., bench/berm height and width) is determined according to the reach of the equipment, dip/shape of the ore body, safety considerations, and most notably rock slope stability. Thus, the slope stability of the open pit is a crucial design factor and has to be considered.

The deterioration of slope stability has severe economic and environmental impacts. Several factors affect the slope stability of open pit such as rock mass strength properties, slope geometry (i.e., overall slope angle and slope extension), presence of groundwater and existence of geological structures (e.g., the plane of weakness, faults, joint sets, etc.). Geological structures determine the slope failure mechanism associated with rock mass and its pattern such as planar, wedge, toppling and/or circular failure [1]-[11]. Therefore, the purpose of this analysis is to evaluate the slope stability of open pit without/with the presence of geological structures (e.g., joint networks). The analysis has been conducted employing shear strength reduction technique (SSRT) implemented in FE analysis.

2. Shear strength reduction technique (SSRT)

In SSRT, the factor of safety is determined from elasto-plastic finite element modelling when using Mohr-Coulomb (MC) failure criterion by artificially weakening/decreasing rock strength properties (i.e., cohesion, c & tangent of friction angle, $\tan\varphi$) in steps/stages until rock slope

Published by the Dnipro University of Technology on behalf of Mining of Mineral Deposits. ISSN 2415-3443 (Online) | ISSN 2415-3435 (Print)

fails/collapses. In the numerical analysis, failure occurs when the converge of the solution could not be reached. The factor of safety (FS) is then taken as the value by which the rock strength has to be reduced to reach failure [12]-[17]. This can be explained mathematically as given in Equation (1) and depicted graphically as illustrated in Figure 1.

$$SRF = \frac{\tan\varphi}{\tan\varphi_f} = \frac{c}{c_f}, \quad (1)$$

where:

SRF – strength reduction factor, which is used to define the value of rock strength parameters at a given stage of the analysis;

c and φ – the rock shear strength input values/parameters (e.g., cohesion and friction angle respectively);

c_f and φ_f – the rock shear strength reduced or mobilized values used in the analysis (e.g., values at which rock slope of open pit will have instability/failure).

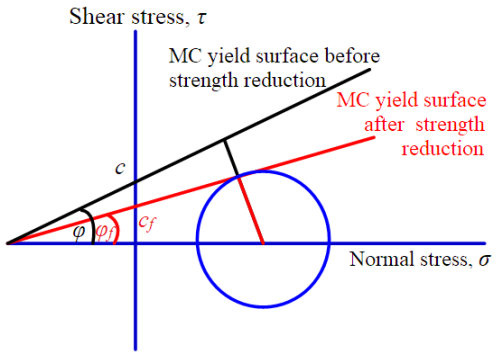

Figure 1. Mohr-Coulomb yield surface/envelope before and after strength reduction (re-plotted after [15])

It is worth noting that SRF is set to 1.0 at the beginning of the calculations (i.e., rock strength properties are set to their input values, c and φ). When failure is reached, SRF corresponds to the value of factor of safety, i.e. [18]:

$$FS = \frac{\tau}{\tau_f}, \quad (2)$$

where:

τ – the actual shear strength of the rock mass slope of open pit and is calculated employing MC criterion:

$$\tau = c + \sigma_n \tan\varphi; \quad (3)$$

τ_f – the shear stress on the sliding/failure surface along two discontinuity plane, and is given by:

$$\tau_f = c_f + \sigma_n \tan\varphi_f; \quad (4)$$

σ_n – the normal stress.

Thus, Equation (2) can be re-written as:

$$FS = \frac{c + \sigma_n \tan\varphi}{c_f + \sigma_n \tan\varphi_f}. \quad (5)$$

One advantage of using FE analysis for evaluating the slope FS is that no assumptions are made regarding the shape or location of the failure surface. Rather, the failure occurs through the zones within the rock mass at which the rock shear strength is unable to resist the applied shear stress [13]. In the current analysis, static dry conditions are assumed considering effective shear strength and deformation parameters, hence ignoring the effects of seismicity and groundwater.

3. Numerical analysis and model set up

Several commercially available FEM codes enable simulating very complex mine geometry efficiently, with the ability to generate discrete fracture networks. Consequently, the SSRT has successfully replaced the conventional limit equilibrium methods in estimating the factor of safety of rock slope. SSRT allows combining slip along joints with failure through intact material. Thus, it offers several advantages in modelling jointed rock mass problems. Also, it allows determining the failure mechanisms without any prior assumptions to its pattern and location[12], [13], [19].

In this study, numerical modelling has been carried out using RocScience RS2D software [20], adopting the elasto-plastic MC yield criterion. The geomechanical properties of all rock masses considered in the analysis are listed in Table 1. Four models have been constructed to evaluate the slope stability of open pit associated with blocky and jointed rock mass.

Table 1. Geomechanical properties of rock mass [20]

Property/rock mass	Upper layer	Coal seam	Lower layer
Density, KN/m^3	22.80	15.50	18.82
E, KPa	75000	2255.12	55100
Poisson's ratio, υ	0.18	0.35	0.22
Cohesion, KPa	29.40	9.80	294.00
Tensile strength, KPa	1300	2750	1500
Friction angle, ϕ	12	5	40
Dilation angle, φ	3.00	1.25	10.00

4. Results and discussion

The following sections present the results of the four modelled cases (i.e., no joints (blocky) rock mass, joint networks parallel to the slope face, parallel joint networks dip out the slope face, and cross-joint networks) in terms of CSRF, maximum total displacement and maximum shear strain.

CSRF has been estimated employing the SSRT. The model geometry was kept the same for all cases considered: slope dimensions (height × width) of 20×30 m; and overall slope angle of 34°) as shown in Figure 2. The applied loading stress field is gravity type considering actual ground surface and $K_0 = 1$ (i.e. $\sigma v = \sigma h$). The results are presented and discussed in terms of CSRF, maximum shear strain and maximum total displacement.

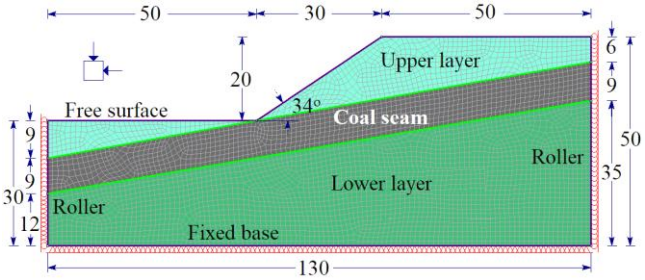

Figure 2. Model geometry (in meters), dimensions and boundary conditions (BCs) – base model

4.1. Case I-no joints existed (blocky) in the rock mass

In this case, the rock slope comprised blocky rock mass in open pit slope. Figure 3 shows the calculated contours of maximum shear strain at the CSRF. The maximum shear strain was found to be 2.338 and occurs at CSRF of 0.65. The contours of the maximum total displacement are displayed in Figure 4, which shows an absolute total displacement of 15.82 m.

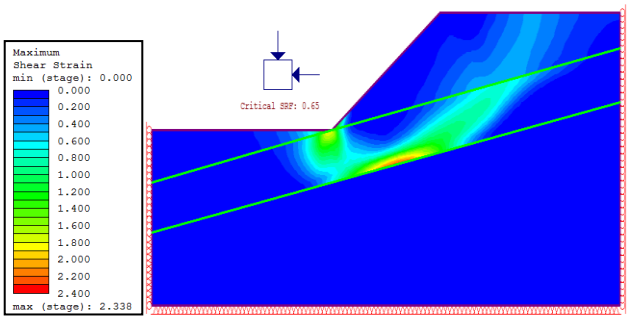

Figure 3. Contours of maximum shear strain (e.g., max. shear strain = 2.338 at CSRF = 0.65)

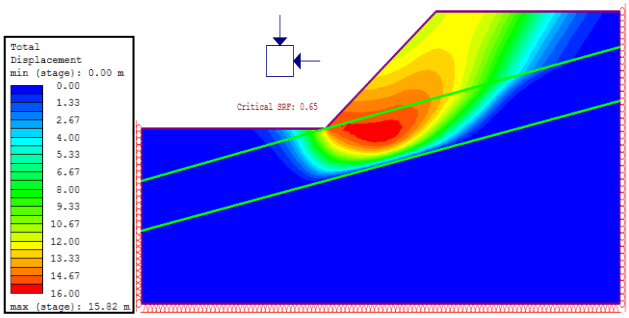

Figure 4. Contours of maximum total displacement (max. displacement = 15.82 m at CSRF = 0.65)

Table 2 gives the maximum shear strain and the maximum total displacements at various strength reduction factors, for this case study.

Table 2. Maximum shear strain and maximum total displacements at various strength reduction factors: case 1 – blocky rock mass

SRF	Max. shear strain	Max. total displacement, m
0.49	0.256	0.00
0.50	0.312	0.40
0.62	1.804	11.63
0.63	2.004	13.13
(CSRF) 0.65	2.338	15.82
0.66	3.984	23.53
0.67	4.318	26.31
0.74	5.337	37.18
0.99	10.792	93.41
1.00	11.267	97.86

Figures 5 and 6 depict the maximum shear strains and maximum total displacements at different SRFs respectively. Figure 5 illustrates that the maximum shear strain increases gradually as strength reduction factor increases till SRF of 0.65, after that, a sharp increase occurs beyond the SRF > 0.65.

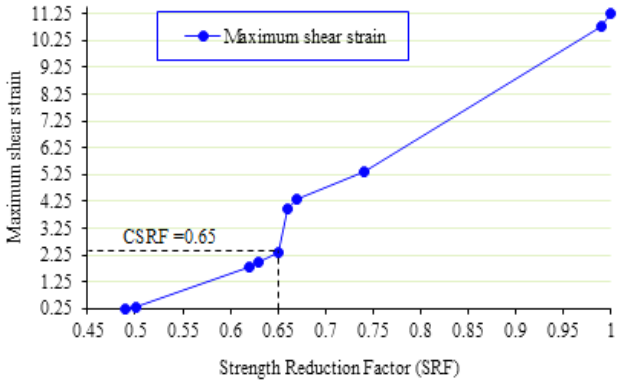

Figure 5. Maximum shear strain at various SRFs

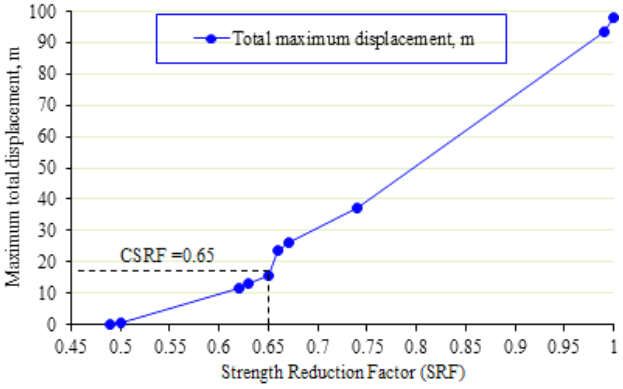

Figure 6. Maximum total displacements at various SRFs

On other meaning, the slope stability eventually deteriorates if the strength properties of the rock mass (c and φ) are decreased to such value where strength reduction factor goes beyond 0.65 and no converge is reached.

Figure 6 yields the maximum total displacement at various SRFs. It can be seen that, as SRF increases, the maximum total displacement slightly increases. The CSRF is 0.65 where maximum total displacement sharply increases to 15.82 m.

4.2. Case II-parallel joint networks to the slope face

In this case, the base model is modified to involve a set of joint networks spaced 5 m apart, parallel and inclined to the slope face at 350 as shown in Figure 7. It also shows the one set parallel joints with the domain of discretization (e.g., meshing). The geomechanical properties (e.g., strength properties) of joint networks are listed in Table 3. Two assumptions have been postulated here; the first one assumed that there is no slip occurred along with joint networks but the second one assumed that joint slip is occurred and followed MC slip criterion.

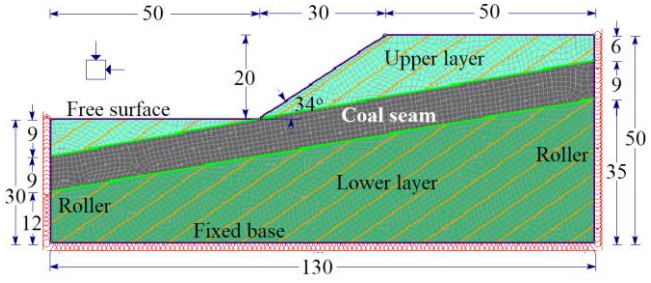

Figure 7. A model set up, meshing and boundary conditions (BCs)-case II (set of parallel joints existed)

Table 3. Geomechanical properties of joint networks

Joint property	
Normal stiffness	250000 MPa/m
Shear stiffness	175000 MPa/m
Initial joint deformation	allowed
Pressure from groundwater analysis	included
Additional pressure inside joint	not included
Slip criterion	no slip allowed MC slip criterion

The results of this analysis, for both two assumptions, are presented and discussed in terms of maximum shear strain and maximum total displacement. Figure 8 depicts the contours of maximum shear strain at CSRF, assuming no slip has occurred to joint sets. The maximum shear strain (e.g., 1.561) occurs when the CSRF, is 0.55 (e.g., less than that obtained in case I-no joints existed). The contours of maximum total displacements are shown in Figure 9. The maximum total displacement is 6.76 m (e.g., less than half of what has been obtained in case I-no joints existed). The maximum shear strain and maximum total displacements at various SRF are listed in Table 4 and plotted as shown in Figures 10 and 11 respectively.

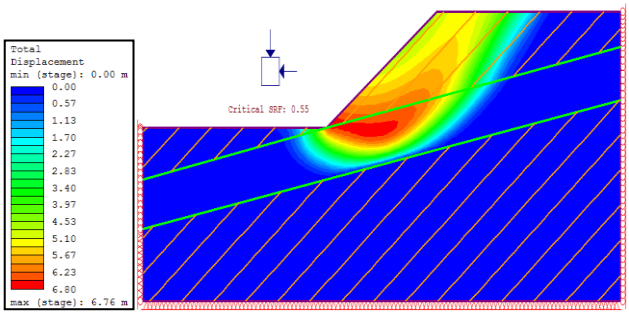

Figure 8. Contours of maximum shear strain (e.g., max. shear strain = 1.561 at CSRF = 0.55)

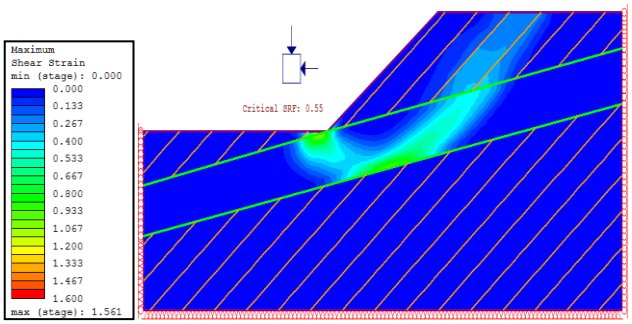

Figure 9. Contours of maximum total displacement (max. displacement = 6.76 m at CSRF = 0.55)

The second assumption (e.g., joint slip occurs and follows MC slip criterion) is modelled. The analysis shows that no iteration convergence reaches. On other meaning, the CSRF is not identified in this case. The maximum shear strain and maximum total displacement at different values of SRFs are listed in Table 5 as well depicted in Figures 12 and 13 respectively. According to these results, the CSRF is 0.49. This simply because abrupt change (e.g., suddenly increase) has occurred beyond that value (e.g., SRF = 0.49) in the values of maximum shear strain and maximum total displacements after that value.

Table 4. Maximum shear strain and maximum total displacements at various strength reduction factors: case II-parallel joint networks existed (no joint slip occurred)

SRF	Max. shear strain	Max. total displacement, m
0.49	0.379	0.00
0.50	0.529	0.80
0.51	0.717	1.84
0.52	0.921	2.98
0.54	1.349	5.43
(CSRF) 0.55	1.561	6.76
0.56	2.019	10.51
0.62	3.625	22.61
0.74	5.980	45.38
0.99	11.629	116.65
1.00	12.468	122.56

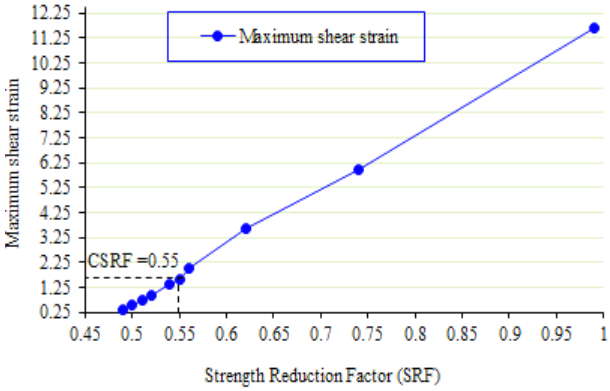

Figure 10. Maximum shear strain at various SRFs

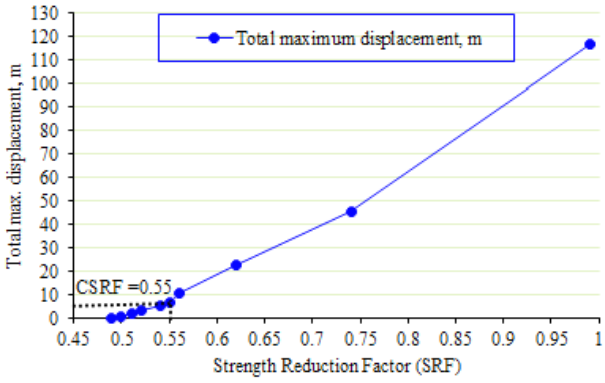

Figure 11. Maximum total displacements at various SRFs

Table 5. Maximum shear strain and maximum total displacements at various strength reduction factors: case II-parallel joint networks existed (MC-joint slip occurred)

SRF	Max. shear strain	Max. total displacement, m
0.01	0.090	0.54
(CSRF) 0.49	0.443	2.21
0.99	10.034	99.13
1.00	10.228	102.31
No CSRF is detected as no convergence occurred in the numerical analysis		

4.3. Case III-parallel joint networks dipping out of slope face

In this case, the base model is modified to include a set of joint networks spaced 5 m apart, parallel and dip out of the slope face at –1350 as shown in Figure 14.

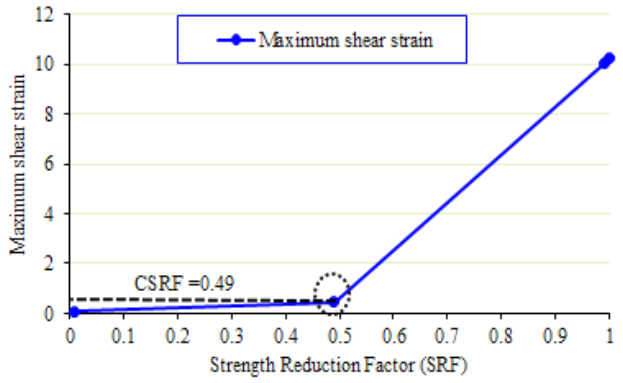

Figure 12. Maximum shear strain at various SRFs (MC joint slip occurs-case II)

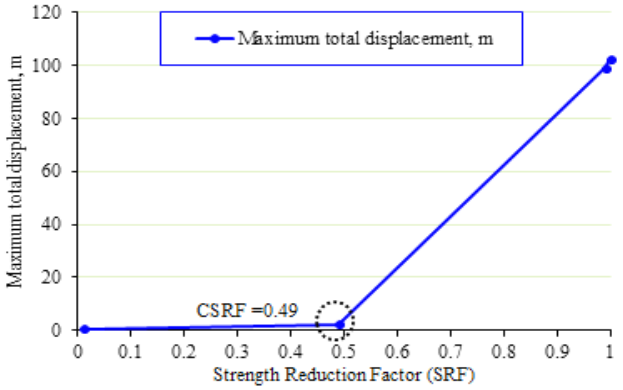

Figure 13. Maximum total displacements at various SRFs (MC joint slip occurs-case II)

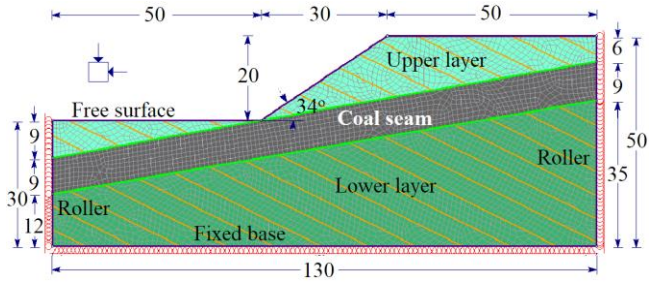

Figure 14. Model set up, meshing and boundary conditions (BCs)-case III (set of parallel joints existed dipping out the slope face)

The contours of maximum shear strain and maximum total displacements at CSRF are shown in Figures 15 and 16 respectively.

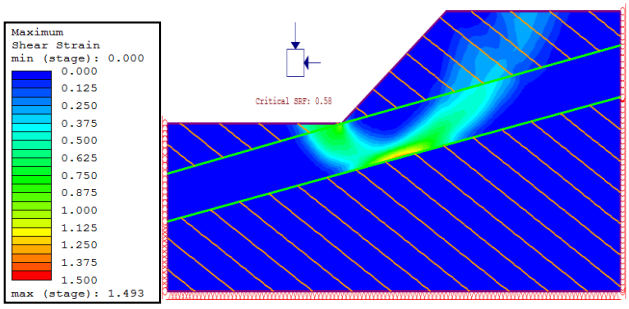

Figure 15. Contours of maximum shear strain (e.g., max. shear strain = 1.493 at CSRF = 0.58)

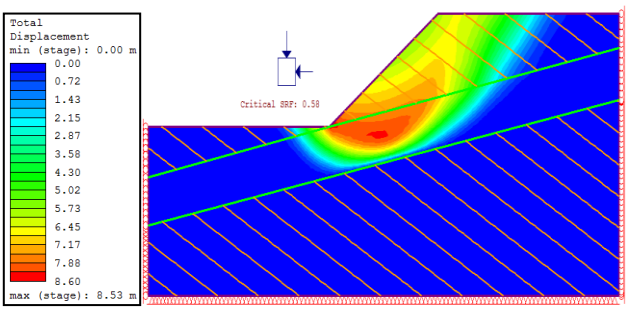

Figure 16. Contours of maximum total displacement (max. displacement = 8.53 m at CSRF = 0.58)

Assuming that there is no joint slip occurs, Figure 15 shows that the maximum shear strain reaches to 1.493 (e.g., little bit small compared with the previous, 1.561) at CSRF of 0.58 (e.g., a little bigger than that obtained when dipping of joints parallel to slope face, 0.55). Also, the contours of maximum total displacements are presented in Figure 16.

The maximum total displacement is found to be 8.53 m at CSRF of 0.58. Hence, only the maximum shear strain becomes smaller when the joint networks dipping out to slope face. However, the maximum total displacement and CSRF become a little bit higher. The maximum shear strain and maximum total displacement at different SRF are given in Table 6, as well as plotted in Figures 17 and 18, for joint networks dipping out to the slope face, respectively.

Table 6. Maximum shear strain and maximum total displacements at various strength reduction factors: case III-joint networks dipping out to slope face (no joint slip occurred)

SRF	Max. shear strain	Max. total displacement, m
0.49	0.328	0.00
0.50	0.432	0.61
0.51	0.566	1.46
0.56	1.203	6.38
0.57	1.361	7.48
(CSRF) 0.58	1.493	8.53
0.59	2.291	12.76
0.62	3.091	17.95
0.74	5.661	38.06
0.99	11.972	109.58
1.00	12.020	112.58

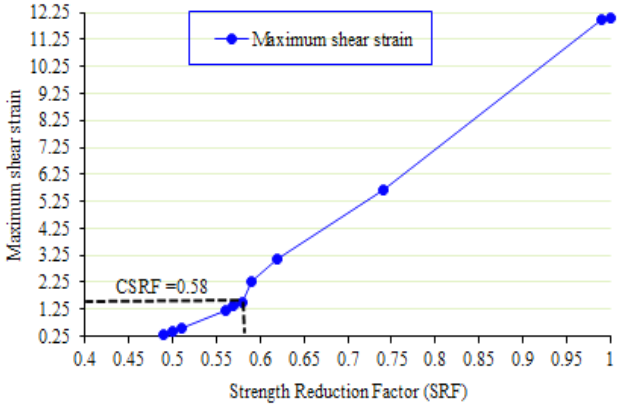

Figure 17. Maximum shear strain at various SRFs (parallel joints dipping out to the slope face)

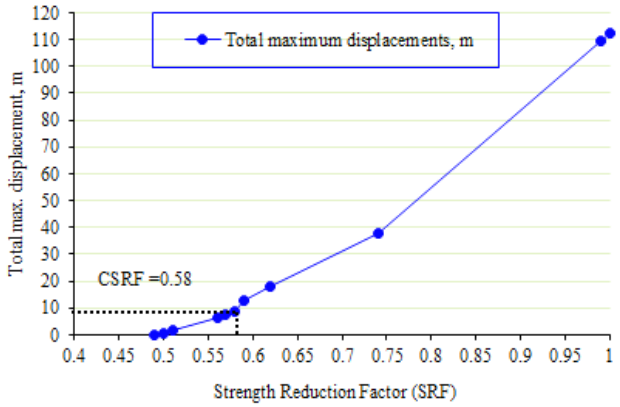

Figure 18. Maximum total displacements at various SRFs (parallel joints dipping out to slope face)

Assuming that, the parallel joint slip occurs and obeys the MC slip criterion. The analysis does not show solution converges. Alternatively, the critical strength reduction factor (CSRF) could not be identified. The maximum shear strain and maximum total displacement at different values of SRFs are listed in Table 7 as well depicted in Figures 19 and 20 respectively. According to the results, the maximum shear strain is 0.554 at CSRF of 0.49 and the maximum total displacement is 1.85 m. This because a sharply increase has occurred beyond that value (e.g., CSRF = 0.49) in the values of maximum shear strain and maximum total displacements after that value.

Table 7. Maximum shear strain and maximum total displacements at various strength reduction factors: case III-joint networks dipping out to slope face (MC-joint slip occurred)

SRF	Max. shear strain	Max. total displacement, m
0.01	0.114	0.54
(CSRF) 0.49	0.554	1.85
0.99	10.236	91.68
1.00	10.317	95.46
No CSRF is defined as solution does not converge		

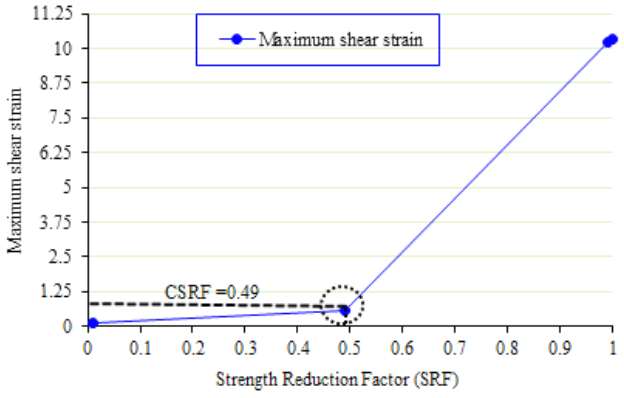

Figure 19. Maximum shear strain at various SRFs (MC joint slip occurs-case III)

4.4. Case IV-cross-joint networks

Here, the base model is modified to involve two set cross-joint networks. These cross-joints provide free surfaces for rotation of the blocks. The two-set cross-joint networks with domain discretization are shown in Figure 21. The geomechanical properties of cross-joints are listed in Table 8.

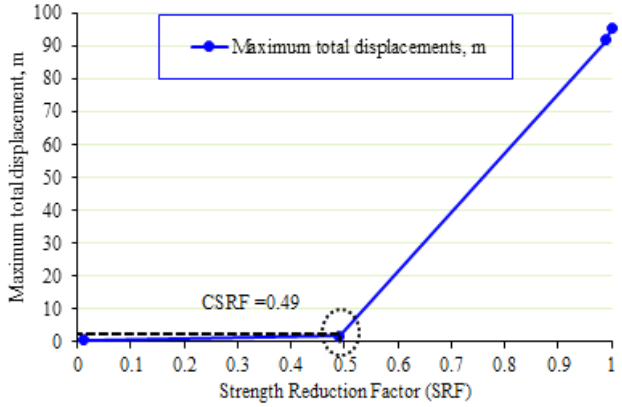

Figure 20. Maximum total displacements at various SRFs (MC joint slip occurs-case III)

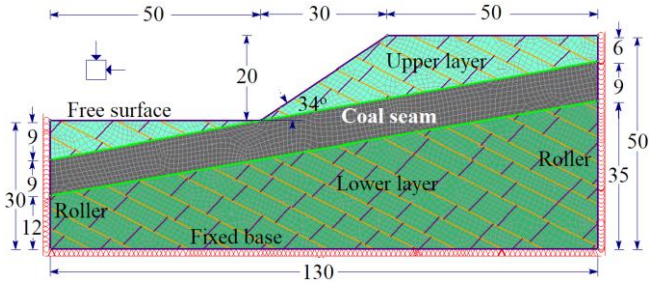

Figure 21. Model geometry shows two set cross-joint networks, meshing and boundary conditions (BCs)

Table 8. Geomechanical properties of cross-joint networks

Joint model	Cross-jointed
Bedding joint property	joint 1
Cross joint property	joint 2
Orientation: use trace plane	yes
Trace plane dip direction	0 deg
Bedding dip	35 deg
Bedding dip direction	135 deg
Cross-joint dip	–55 deg
Cross-joint dip direction	135 deg
Bedding spacing mean	5 m
Bedding spacing distribution	normal
Bedding spacing std. dev.	1 m
Bedding spacing rel. min.	3 m
Bedding spacing rel. max.	3 m
Cross-joint spacing mean	10 m
Cross-joint spacing distribution	normal
Cross-joint spacing std. dev.	2 m
Cross-joint spacing rel. min.	6 m
Cross-joint spacing rel. max.	6 m
Joint ends	all closed

The maximum shear strain and the maximum total displacement contours are shown in Figures 22 and 23 respectively. Figure 22 shows that the maximum shear strain reaches to 0.707 when CSRF was 0.53, while the maximum total displacement becomes 4.03 m as depicted in Figure 23.

The maximum shear strain and maximum total displacement at different SRFs are listed in Table 9, as well as plotted in Figures 24 and 25, for cross-joint networks, respectively.

It can be seen that the maximum shear strain reaches 0.707 and the maximum total displacement becomes 4.03 m at CSRF of 0.53.

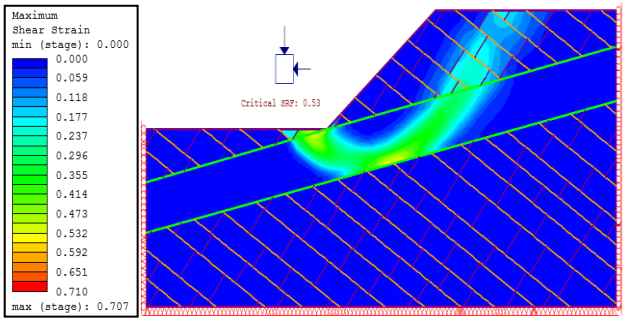

Figure 22. Contours of maximum shear strain (e.g., max. shear strain = 0.707 at CSRF = 0.53)

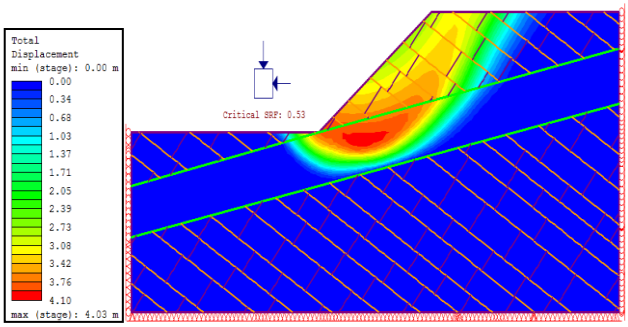

Figure 23. Contours of maximum total displacement (max. displacement = 4.03 m at CSRF = 0.53)

Table 9. Cross-joints networks at different strength reduction factors (no joint slip occurred)

SRF	Max. shear strain	Max. total displacement, m
0.49	0.301	0.00
0.50	0.387	0.62
0.51	0.506	1.63
0.52	0.607	2.80
(CSRF) 0.53	0.707	4.03
0.54	1.451	7.83
0.56	1.719	9.86
0.62	3.110	23.37
0.74	6.323	48.32
0.99	12.743	125.50
1.00	13.101	127.69

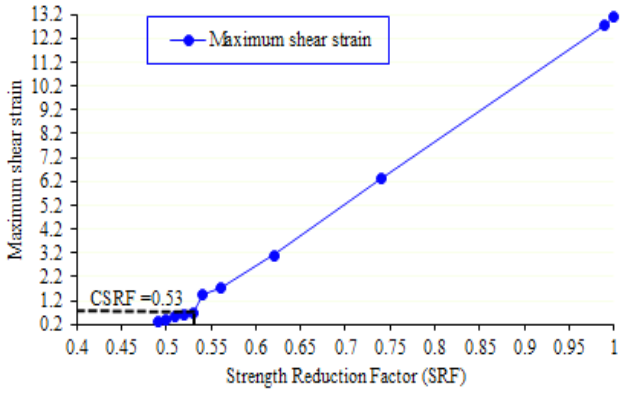

Figure 24. Maximum shear strain at various SRFs (cross-joint networks)

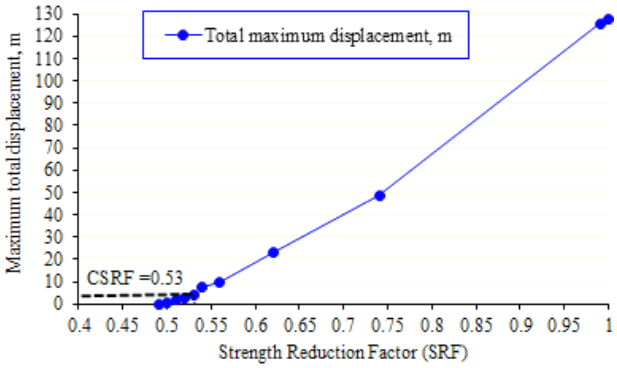

Figure 25. Maximum total displacements at various SRFs (cross-joint networks)

Alternatively, there is no converge that exists after CSRF of 0.53. Table 10 introduces the values of maximum shear strain and maximum total displacement at different SRFs, as well as depicted in Figures 26 and 27 respectively, assuming the joint slip has taken place. It can be seen that CSRF is found to be 0.49 after which no solution could be identified by numerical modelling analysis.

Table 10. Maximum shear strain and maximum total displacements at various strength reduction factors: case IV-cross-joint networks (MC-joint slip occurred)

SRF	Max. shear strain	Max. total displacement, m
0.01	0.144	0.56
(CSRF) 0.49	0.423	2.06
0.99	11.316	104.96
1.00	11.494	107.10
No CSRF is detected as no converge occurred		

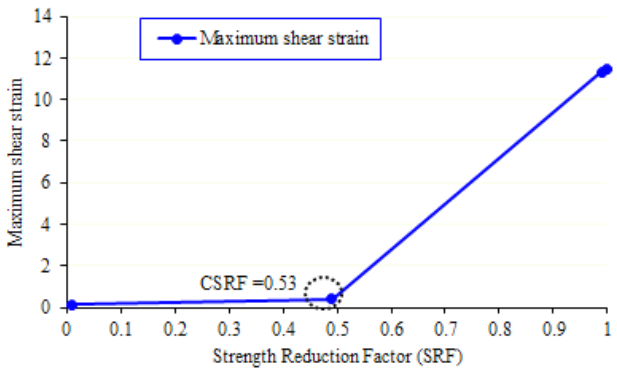

Figure 26. Maximum shear strain at various SRFs (MC joint slip occurs-case IV)

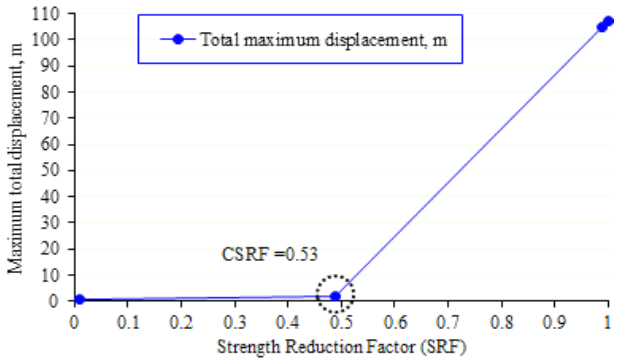

Figure 27. Maximum total displacements at various SRFs (MC joint slip occurs-case IV)

5. Conclusions

The slope stability of rock mass is significant to design parameters in open pit mines. Unexpected instability is eventually costly, hazardous to personnel/machinery, disrupted to the mining operation and time-consuming. Many factors are influencing the slope stability such as slope geometry, rock mass properties, overall slope angle, presence of groundwater and existence of geological structures/discontinuities. The latter factor was considered the focus of this study. Geological structures (e.g., discontinuities/joints) weaken the strength of rock mass slope (e.g., increases the rock mass deformability). Thus, this study aims to evaluate the slope stability of rock mass associated with joints networks. Shear strength reduction technique (SSRT), based finite element (FEM), has been adopted in this analysis. The SSRT reduces the shear strength parameters (c, φ) of rock mass in stages until the slope fails/collapses (e.g., numerically no convergence in solution is reached).

Four cases have been studied and analyzed; the first model comprises blocky rock mass while a network of parallel joints exists in the second model (e.g., parallel to slope face), the third model includes a parallel joint networks dip out to the slope face and the last model involves two sets of cross-joint networks. The slope stability, for the four modelled cases, is evaluated in terms of CSRF, maximum shear strain and absolute total displacement. Maximum shear strain gives a good insight into affected zones where slip takes place. The CSRF indicates whether the slope face is stable (CSRF ≥ 1) or not. The minimum CSRF (e.g., CSRF = 0.53 compared to 0.55 for parallel joints dip out to the slope face, 0.58 for joints parallel to slope face and 0.65 with no joint existed) is obtained with cross-joints network existed. The CSRF (e.g., CSRF = 0.49) reduces when the MC slip criterion is adopted with the jointed rock mass. The CSRF, maximum shear strain and total displacement for all modelled cases are depicted in Figure 28 as well listed in Table 11 below.

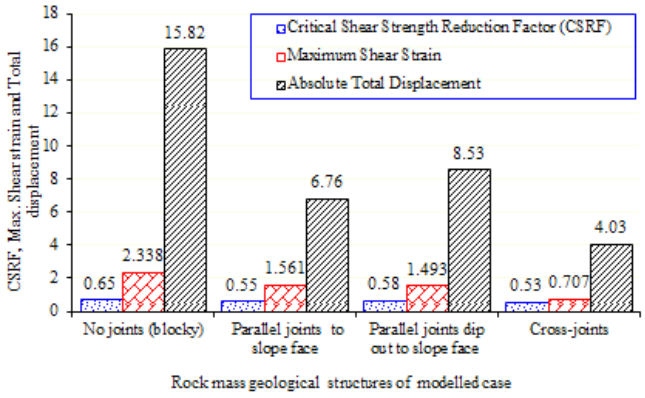

Figure 28. Stability indicators with respect to existence of geological discontinuities

Table 11. Summary of the numerical analysis results for different modelled cases

Modelled case	CSRF	Max shear strain	Absolute total displacement
No joints (blocky) associated	0.65	2.338	15.82
Parallel joints to slope face	0.55	1.561	6.76
Parallel joints dip out to slope face	0.58	1.493	8.53
Cross-joints	0.53	0.707	4.03

Acknowledgements

The authors acknowledge the support of Rocscience Inc. for getting a free full educational version of RS2D (Rock-Soil two-dimensional finite-element analysis program). The authors are grateful for their support.

References

[1] Jaeger, J.C. (1971). Friction of rocks and stability of rock slopes. *Géotechnique*, *21*(2), 97-134. https://doi.org/10.1680/geot.1971.21.2.97
[2] Hoek, E., & Bray, J.W. (1981). *Rock slope engineering*. London, United Kingdom: Institution of Mining and Metallurgy.
[3] Gray, P.A. (1988). *Slope stability considerations of a major excavation in rock: the Mt Newman case study*. Ph.D. Thesis. Wollongong, New South Wales, Australia: University of Wollongong.
[4] Goodman, RE. (1989). *Introduction to rock mechanics*. New York, United States: Wiley.
[5] Bye, A., & Bell, F. (2001). Stability assessment and slope design at Sandsloot open pit, South Africa. *International Journal of Rock Mechanics and Mining Sciences*, *38*(3), 449-466. https://doi.org/10.1016/s1365-1609(01)00014-4
[6] Wyllie, D.C., & Mah, C.W. (2017). *Rock slope engineering*. London, United Kingdom: Spon Press. https://doi.org/10.4324/9780203499085
[7] Hossain, M. (2011). *Stability analysis of anchored rock slopes against plane failure subjected to surcharge and seismic loads*. M. Eng. Thesis. Perth, Australia: Edith Cowan University.
[8] Li, A.J., Merifield, R.S., & Lyamin, A.V. (2011). Effect of rock mass disturbance on the stability of rock slopes using the Hoek–Brown failure criterion. *Computers and Geotechnics*, *38*(4), 546-558. https://doi.org/10.1016/j.compgeo.2011.03.003
[9] Marndi, B. (2011). *Stability of slopes in iron ore mines*. B. Eng. Thesis. Rourkela, India: Deemed University, National Institute of Technology.
[10] Fleurisson, J.A., & Cojean, R. (2014). Error reduction in slope stability assessment. *Surface Mining Methods, Technology and Systems*, (1), 1-41.
[11] Kumar, V., & Parkash, V. (2015). A model study of slope stability in mines situated in south India. *Advances in Applied Science Research*, *6*(8), 82-90.
[12] Dawson, E.M., Roth, W.H., & Drescher, A. (1999). Slope stability analysis by strength reduction. *Géotechnique*, *49*(6), 835-840. https://doi.org/10.1680/geot.1999.49.6.835
[13] Griffiths, D.V., & Lane, P.A. (1999). Slope stability analysis by finite elements. *Géotechnique*, *49*(3), 387-403. https://doi.org/10.1680/geot.1999.49.3.387
[14] Hammah, R., Yacoub, T., Corkum, B., Wibowo, F., & Curran, J. (2007). Analysis of blocky rock slopes with finite element Shear Strength Reduction analysis. *Rock Mechanics: Meeting Society's Challenges and Demands*, 329-334. https://doi.org/10.1201/noe0415444019-c40
[15] Chatterjee, P., & Elkadi, A. (2012). *Strength reduction analysis*. Delft, The Netherlands: TNO DIANA BV.
[16] Soren, K., Budi, G., & Sen, P. (2013). Stability analysis of open pit slopes in jointed rock mass by finite element method. *Proceedings of Indian Geotechnical Conference*, 1-9.
[17] Berisavljević, Z., Berisavljević, D., Čebašek, V., & Rakić, D. (2015). Slope stability analyses using limit equilibrium and strength reduction methods. *Građevinar*, *67*(10), 975-983. https://doi.org/10.14256/JCE.1030.2014
[18] Soren, K., Budi, G., & Sen, P. (2014). Stability analysis of open pit slope by finite difference method. *International Journal of Research in Engineering and Technology*, *03*(05), 326-334. https://doi.org/10.15623/ijret.2014.0305062
[19] Matsui, T., & San, K.-C. (1992). Finite element slope stability analysis by shear strength reduction technique. *Soils and Foundations*, *32*(1), 59-70. https://doi.org/10.3208/sandf1972.32.59
[20] RocScience Inc. (2016). *RS2D (Rock and Soil 2-dimensional analysis program)*. Toronto, Canada: 439 University Ave. Ste 780, Ontario M5G 1Y8.

Аналіз стійкості укосу гірського масиву методом зменшення опору зсуву

В.Р. Абделах, М.Ю. Хусейн, С.С. Імбабі

Мета. Дослідження стійкості укосу при відкритій розробці вугільного пласта в умовах твердих і тріщинуватих порід на основі чисельного моделювання.

Методика. Функція плинності Мора-Кулона і метод зменшення опору зсуву використані разом з аналізом кінцевих елементів, причому 4 укоси з відмінностями в геометрії та геологічних структурних характеристиках (з оптимальним кутом схилу 34°) проаналізовані за допомогою двомірної програми FEA Program RS2D. Перший укіс представлений бриластою гірської породою, другий укіс покритий сіткою тріщин, паралельних поверхні укосу, третій укіс має паралельні тріщини, перпендикулярні до поверхні укосу, і останній укіс покритий сіткою пересічних тріщин.

Результати. Показано, що ступінь стійкості укосу характеризується індексом зменшення критичного опору (ІЗКО) і при ІЗКО ≥ 1 укіс вважається стійким. Встановлено, що мінімальне значення ІЗКО дорівнює 0.53 (0.55 – для паралельних тріщин, перпендикулярних до поверхні укосу; 0.58 – для тріщин паралельних поверхні укосу; 0.65 – при відсутності тріщин) і відповідає укосу, який покритий сіткою пересічних тріщин. ІЗКО зменшується (наприклад, до 0.49), коли зсувне зміщення функції плинності Мора-Кулона застосовується для аналізу тріщинуватих порід.

Наукова новизна. Запропоновано індекс зменшення критичного опору в якості нового індикатора стійкості, який є ключовим фактором методу зменшення опору зсуву, заснованого на методі скінченних елементів, і застосовується для виявлення геологічних несуцільностей укосу кар'єру.

Практична значимість. Запропоновано метод зменшення опору зсуву при оцінці стійкості схилу в кар'єрах з урахуванням існуючих геологічних особливостей. Стійкість породного масиву є важливим фактором при проектуванні параметрів кар'єрів, а при проектуванні шахт – для вибору місць та способів кріплення.

Ключові слова: *стійкість укосу кар'єру, метод зменшення опору зсуву„ фактор безпеки, індекс зменшення критичного опору*

Анализ устойчивости откоса горного массива методом уменьшения сопротивления сдвигу

В.Р. Абделлах, М.Ю. Хуссейн, С.С. Імбаби

Цель. Исследование устойчивости откоса при открытой разработке угольного пласта в условиях твердых и трещиноватых пород на основе численного моделирования.

Методика. Функция текучести Мора-Кулона и метод уменьшения сопротивления сдвигу использованы вместе с анализом конечных элементов, причем 4 откоса с различиями в геометрии и геологических структурных характеристиках (с оптимальным углом склона 34°) проанализированы с помощью двухмерной программы FEA Program RS2D. Первый откос представлен глыбистой горной породой, второй откос покрыт сеткой трещин, параллельных поверхности откоса, третий откос имеет параллельные трещины, перпендикулярные к поверхности откоса, и последний откос покрыт сеткой пересекающихся трещин.

Результаты. Показано, что степень устойчивости откоса характеризуется индексом уменьшения критичного сопротивления (ИУКС) и при ИУКС ≥ 1 откос считается устойчивым. Установлено, что минимальное значение ИУКС равно 0.53 (0.55 – для параллельных трещин, перпендикулярных к поверхности откоса; 0.58 – для трещин, параллельных поверхности откоса; и 0.65 – при отсутствии трещин) и соответствует откосу, который покрыт сеткой пересекающихся трещин. ИУКС уменьшается (например, до 0.49), когда сдвиговое смещение функции текучести Мора-Кулона применяется для анализа трещиноватых пород.

Научная новизна. Предложен индекс уменьшения критичного сопротивления в качестве нового индикатора устойчивости, который является ключевым фактором метода уменьшения сопротивления сдвигу, основанного на методе конечных элементов, и применяется для выявления геологических несплошностей откоса карьера.

Практическая значимость. Предложен метод уменьшения сопротивления сдвигу при оценке устойчивости склона в карьерах с учетом существующих геологических особенностей. Устойчивость породного массива является важным фактором при проектировании параметров карьеров, а при проектировании шахт – для выбора места и способов крепления.

Ключевые слова: *устойчивость откоса карьера, метод уменьшения сопротивления сдвигу, фактор безопасности, индекс уменьшения критичного сопротивления*

Article info

Received: 22 September 2019
Accepted: 20 March 2020
Available online: 18 April 2020